Bulletin of the Seismological Society of America, Vol. 102, No. 2, pp. 900–908, April 2012, doi: 10.1785/0120110151

Ⓔ

Short Note

Comparisons of Triggered Tremor in California

by Kevin Chao, Zhigang Peng, Amanda Fabian, and Lujendra Ojha

Abstract We conduct a visual inspection of deep nonvolcanic tremor triggered by large teleseismic earthquakes around the Calaveras fault in northern California (NC) and the San Jacinto fault in southern California (SC). Out of the 42 large ($M_w \geq 7.5$) earthquakes between 2001 and 2010, only the 2002 M_w 7.9 Denali fault earthquake triggered clear tremor in these two regions. This is in marked contrast with the Parkfield–Cholame section of the San Andreas fault in central California (CC), where 12 earthquakes have triggered tremor in that region. The amplitude of the triggered tremor correlates with that of the triggering surface waves in CC and is consistent with the clock-advance model. The lack of widespread triggered tremor in NC and SC is not simply a consequence of their different background noise levels from CC, but rather reflects different background tremor rates in these regions.

Online Material: Tables of parameters for triggered/nontriggered teleseismic earthquakes and triggered tremors, and figures of band-pass-filtered seismograms, maximum vertical PGVs versus median amplitude of band-pass-filtered envelope functions, tremor amplitude versus PGV, and *S*-wave spectra (and corresponding noise) of local selected earthquakes.

Introduction

Deep nonvolcanic tremor has been recorded along many major plate boundary faults, indicating that they are more common than previously thought (Peng and Gomberg, 2010; Beroza and Ide, 2011, and references therein). While most tremor occurs spontaneously with or following slow-slip events (Rogers and Dragert, 2003; Obara *et al.*, 2004), tremor can also be triggered by large distant earthquakes and is known as "triggered tremor" (Miyazawa and Mori, 2006; Rubinstein *et al.*, 2007). Although triggered and ambient (i.e., not triggered) tremor share many similarities (Shelly *et al.*, 2011), the fundamental mechanism of triggered tremor and their relationship with slow-slip events remains unclear (Beroza and Ide, 2009).

Gomberg (2010) proposed a clock-advance model assuming that triggered tremor occurs on the same patch of ambient tremor and that their duration time is advanced by the passing surface waves. In this model, the perturbed seismicity rate r is proportional to the background rate r_0, and a function is used to describe how the failure time of a fault patch is advanced by the perturbing stress. Hence, the model predicts that larger triggering waves would result in larger triggered tremor signals and that triggered tremor is more abundant when r_0 is larger. Both Rubinstein *et al.* (2009) and Gomberg (2010) examined triggered tremor in Cascadia and inferred that the tremor-triggering potential is higher during an episodic tremor-and-slip (ETS) event or intensive tremor sequence, which is consistent with the predictions of the clock-advance model. However, Gomberg (2010) examined the relationship between the amplitudes of the triggering waves and triggered tremor for four observations in Cascadia (Rubinstein *et al.*, 2009), and the obtained results do not match the predictions of the clock-advance model. In comparison, Chao *et al.* (2012) found a positive relationship between the amplitudes of surface waves from nine teleseismic earthquakes and those of triggered tremor beneath the Central Range in Taiwan. Miyazawa and Brodsky (2008) observed an exponential relationship between the triggered tremor amplitude and the dynamic stress at the source region in southwest Japan. Those diverse observations suggest more studies are needed to understand the relationship between the triggering wave, triggered tremor, and background tremor rate.

An ideal region to examine the relationship between triggering waves and tremor characteristics is the Parkfield–Cholame section of the San Andreas fault (SAF) in central California (CC), where many triggered (Gomberg *et al.*, 2008; Peng *et al.*, 2008; Ghosh *et al.*, 2009; Peng *et al.*, 2009; Guilhem *et al.*, 2010; Shelly *et al.*, 2011) and ambient (Nadeau and Dolenc, 2005; Nadeau and Guilhem, 2009) tremors have been recorded. In comparison, in northern California (NC) and southern California (SC), the only clear

case of teleseismically triggered tremor reported so far is from the 2002 M_w 7.9 Denali fault earthquake (Gomberg *et al.*, 2008; Fabian *et al.*, 2009; Wang and Cochran, 2009). It is not yet clear whether such a difference is caused by different observational capabilities (e.g., different instrumentation, background noise level) or different conditions that favor tremor generation in these regions.

In this study, we conduct a systematic search in NC and SC for tremor triggered by large teleseismic events between 2001 and 2010. We focus on the regions around the central segment of the Calaveras fault (CF) in NC (Fig. 1a) and the Anza segment of the San Jacinto fault (SJF) in SC (Fig. 1b), where tremor was triggered by the Denali fault earthquake (Gomberg *et al.*, 2008). A total of 12 tremor-triggering events in CC (Peng *et al.*, 2009; Peng *et al.*, 2010; Shelly *et al.*, 2011) were used for comparison with the results in NC and SC in the same time period. In addition, we measure the background noise level and quantify the triggering threshold in each region. Finally, we explore possible reasons that explain the lack of triggered tremor observations in NC and SC.

Data and Analysis Procedure

In this study, we first selected 42 earthquakes from the Advanced National Seismic System (ANSS) earthquake catalog between 2001 and 2010; all had moment magnitude $M_w \geq 7.5$, hypocentral depth < 100 km, and epicentral distance > 1000 km from the broadband station PKD in CC (Ⓔ Table S1, available as an electronic supplement to this paper). Except for time range, the other search criteria are the same as used in Peng *et al.* (2009). Next, we acquired seismic data spanning five hours before and after the origin time of each teleseismic event at all available stations in NC and SC. In CC, we used the results from the 31 earthquakes analyzed in Peng *et al.* (2009) and requested the seismic data for 11 additional events since June 2008.

Following Peng *et al.* (2009), we visually identified triggered tremor as bursts of high-frequency (2–8 Hz), nonimpulsive signals that are coherent among many nearby stations and correlate with the timing of the surface waves from the teleseismic earthquakes (e.g., Fig. 2). We used the following criteria to identify triggered tremor. First, the high-frequency tremor bursts were associated with the periods of surface waves and were recorded by at least five surrounding stations within 100 km of the potential triggered tremor source. Second, the move-out patterns (i.e. later arrivals with increasing distances) of tremor bursts (Fig. 2) were used to further confirm the positive triggering cases. Figure 2 shows a case in which triggered tremor was identified in NC and SC after the 2002 M_w 7.9 Denali fault earthquake.

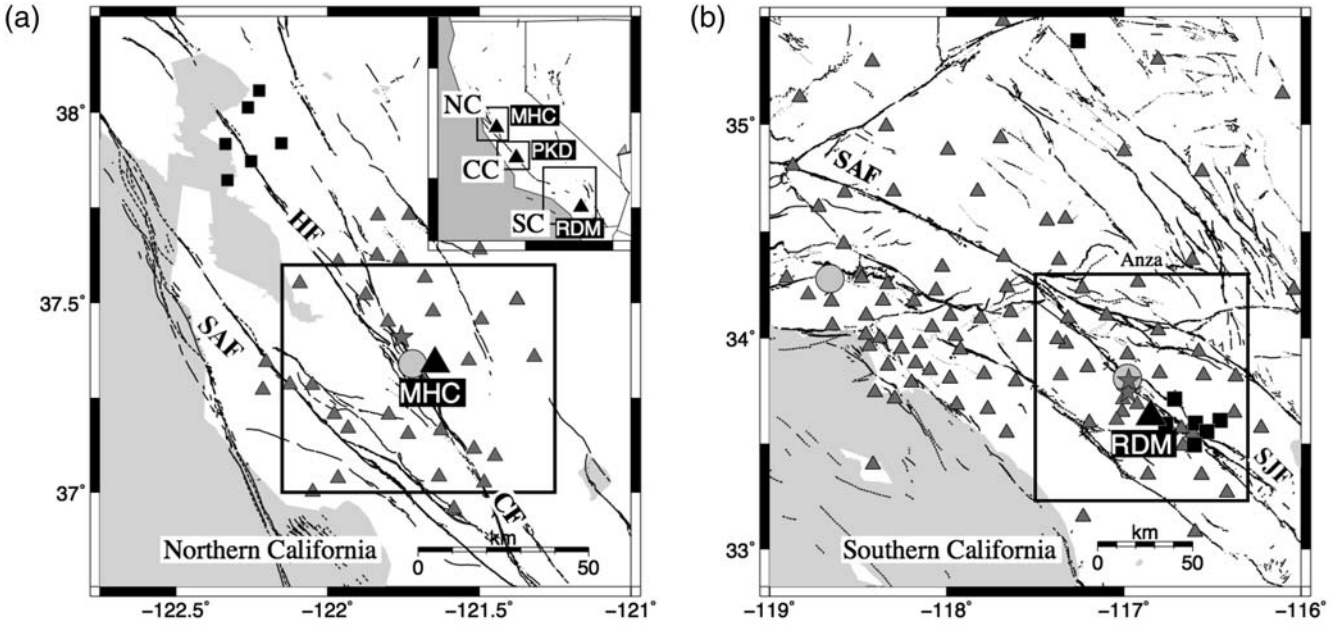

Figure 1. (a) Map of the study region in northern California (NC). Small triangles, short-period stations belonging to the Northern California Seismic Network (NCSN); black squares, the borehole stations in the Northern Hayward Fault Network (NHFN); large black triangle, broadband station MHC; black lines, the active faults of Calaveras fault (CF), San Andreas fault (SAF), and Hayward fault (HF); gray circle, location of the tremor triggered by the 2002 M_w 7.9 Denali fault earthquake (Gomberg *et al.*, 2008). The two local earthquakes used to demonstrate the path or site effects (Ⓔ Fig. S4, available as an electronic supplement to this paper) are close to each other and are marked by a dark gray star. The insert indicates the study region in NC, central California (CC), and southern California (SC). The broadband stations MHC, PKD, and RDM are marked by small black triangles in NC, CC, and SC, respectively. (b) Study region in southern California. Black lines, active faults of San Jacinto fault (SJF) and SAF; gray triangles, broadband stations belonging to the Caltech (CI) and Anza (AZ) network; black squares, borehole stations belong to the Plate Boundary Observatory (PBO); gray circles, previously determined tremor locations triggered by the Denali earthquake (Gomberg *et al.*, 2008). The dark gray stars mark two local earthquakes used to demonstrate the path or site effects (Ⓔ Fig. S4, available as an electronic supplement to this paper).

Figure 3 demonstrates one nontriggering example without coherence signals by the 2007 M_w 8.1 Kuril Island earthquake in NC and SC. Figure 4 shows another example in which triggered tremor could not be identified following the 2010 M_w 8.8 Chile earthquake. In this case, we used a higher frequency band of 10 Hz, high-pass-filtered in NC and SC, respectively, in order to remove potential contamination of earthquake signals from the Coso geothermal fields triggered by the Chile mainshock (Peng *et al.*, 2010; Ⓔ Fig. S1, available as an electronic supplement to this paper).

Triggered Tremor in California

Among all 42 events, the 2002 M_w 7.9 Denali fault earthquake is the only event that has triggered tremor in NC and SC (Fig. 2), which is in marked contrast with the observations of 12 telesesmic earthquakes that triggered tremor (including the Denali fault event) in CC. This perhaps is not surprising, because the Denali fault earthquake produced the largest peak ground velocity (PGV) at all regions (Fig. 5). However, the 2007 M_w 8.1 Kuril Island earthquake also triggered tremor in CC (Peng *et al.*, 2009) but not in NC and SC (Fig. 3). Similarly, the 2010 Chile earthquake triggered clear tremor in CC (Peng *et al.*, 2010) but did not trigger any tremor in NC or SC (Fig. 4). Although there were some high-frequency spikes at a few stations during the timing of the surface waves, these signals are not coherent at nearby stations and hence are not classified as triggered tremor.

Tremor triggered by the Denali fault earthquake has been analyzed in several previous studies (Gomberg *et al.*, 2008; Peng *et al.*, 2008; Peng *et al.*, 2009). Here we used the tremor locations triggered by the Denali fault earthquake along the CF in NC (121.72° W, 37.34° N, 15 km in depth) and the SJF in SC (116.98° W, 33.81° N, 14 km in depth; Gomberg *et al.*, 2008) and shifted the tremor bursts and nearby surface waves back to the tremor source region to further examine their relationships. In both regions, the tremor was initiated in the first few cycles of the Love waves when it

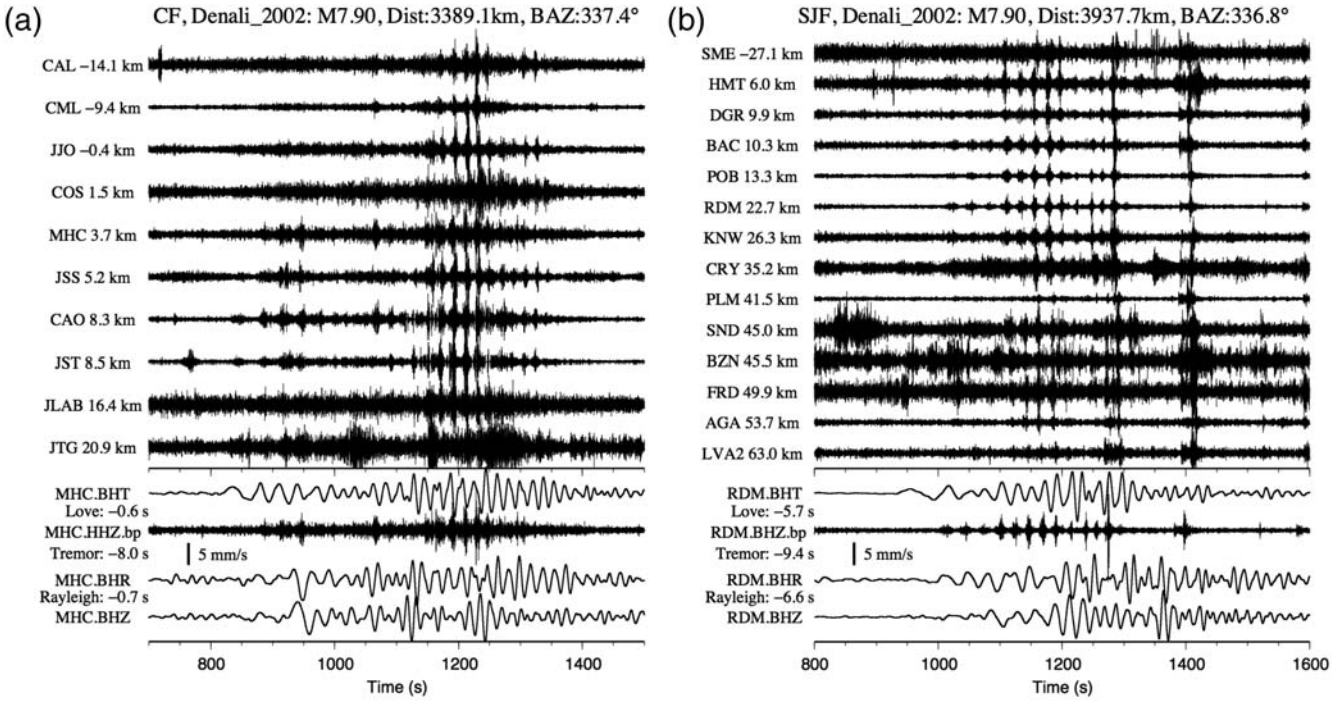

Figure 2. (a) Top: 2–8-Hz band-pass-filtered vertical seismograms showing the move-out of tremor along the Calaveras fault (CF) in northern California (NC) triggered by the 2002 M_w 7.9 Denali fault earthquake. The seismograms are plotted along the strike of the CF, with northwest at the top and southeast on the bottom. The along-strike distance to the tremor source and the station names are marked by the seismograms. The event name and the occurrence year, its magnitude (M), and the epicenter distance (Dist) and back azimuth (BAZ) relative to the broadband station are shown above the siesmograms. Bottom: A comparison between the instrument-corrected transverse (BHT), radial (BHR), and vertical (BHZ) velocity seismograms and the 2–8-Hz band-pass-filtered seismogram recorded at the broadband station MHC. The zero time corresponds to the origin time of the mainshock. The velocity seismograms have been time-shifted back to the tremor sources. The adjusted times of Love waves (in the T component), Rayleigh waves (in the R and Z components), and tremor are marked below the station names. The thick vertical bar marks the amplitude scale of surface waves. (b) Top: 2–8-Hz band-pass-filtered vertical seismograms showing the move-out of tremor triggered by the Denali fault earthquake along the San Jacinto fault (SJF) in the Anza network in southern California (SC). The seismograms are plotted along the strike of the SJF, with northwest at the top and southeast on the bottom. Bottom: A comparison between the velocity and the 2–8-Hz band-pass-filtered seismograms recorded at the broadband station RDM. Other notations are the same as in Figure 2a.

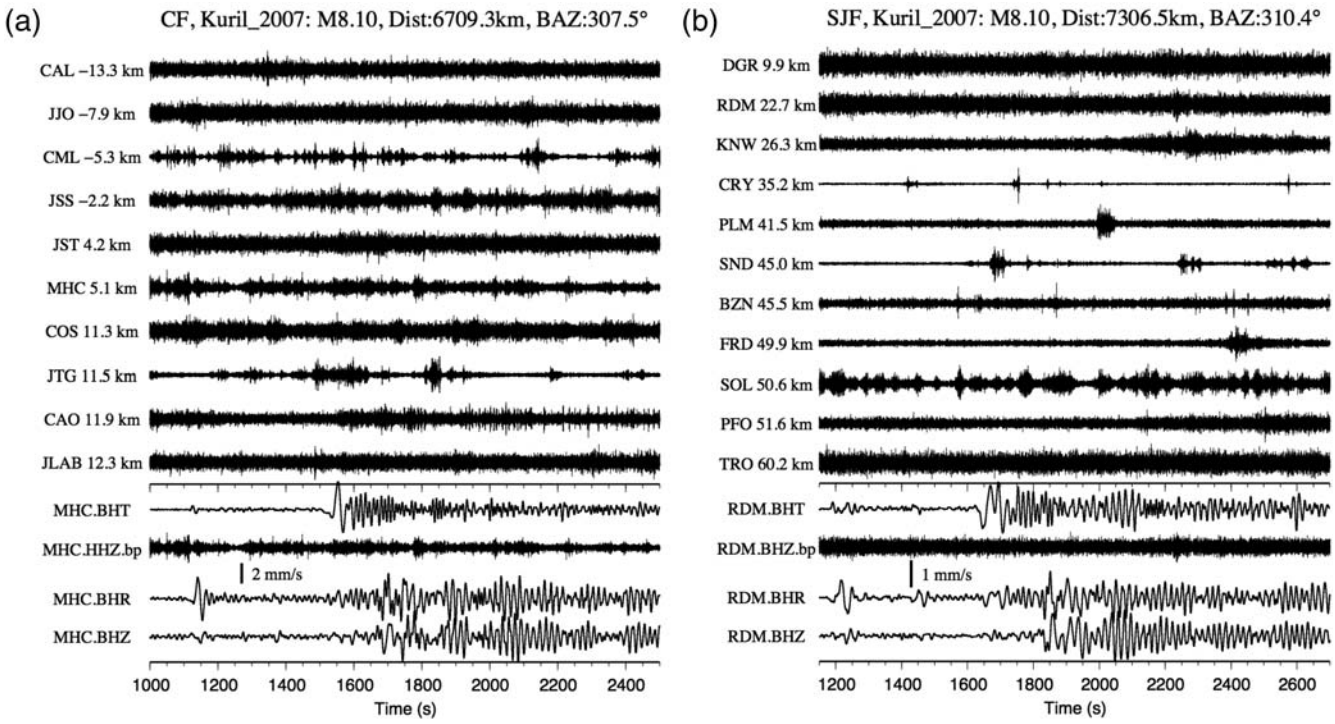

Figure 3. 2–8-Hz band-pass-filtered seismograms showing no tremor triggered by the 2007 M_w 8.1 Kuril Island earthquake at (a) the Calaveras fault (CF) in NC and at (b) the San Jacinto fault (SJF) in SC. Other notations are the same as in Figure 2.

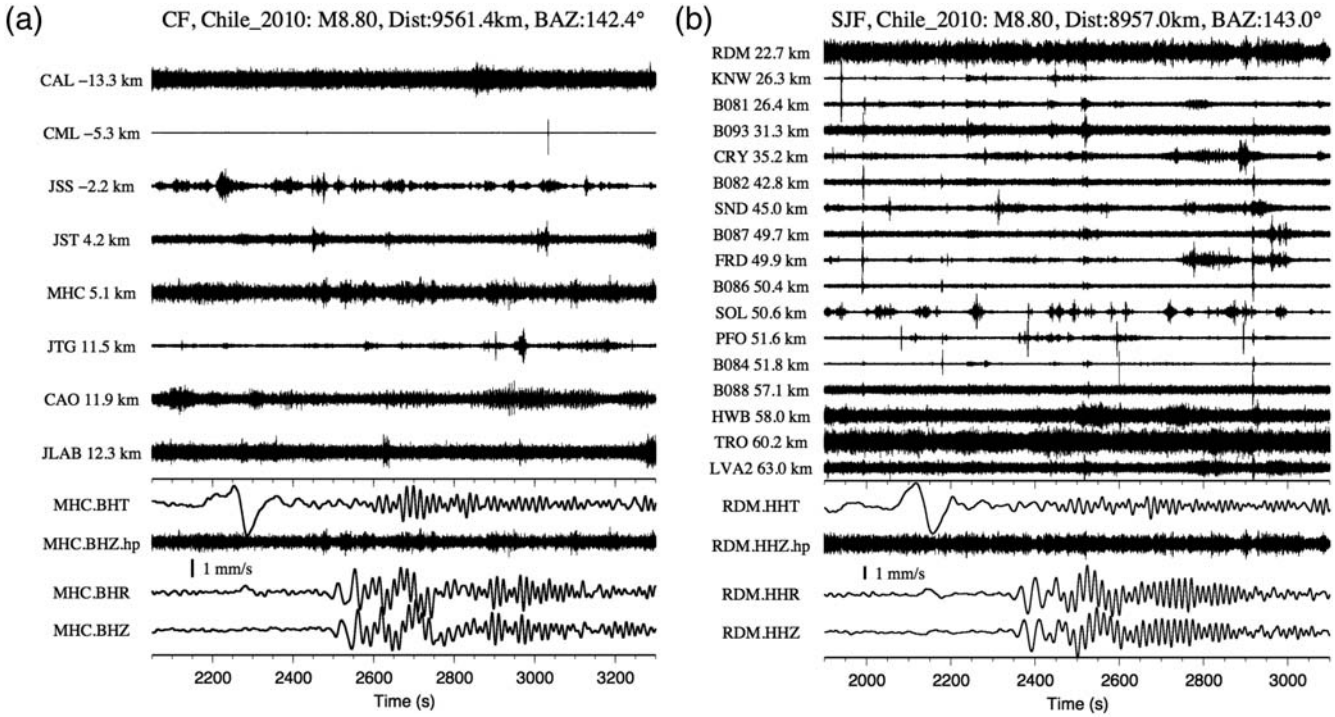

Figure 4. 10-Hz high-pass-filtered seismograms showing no tremor triggered by the 2010 M_w 8.8 Chile earthquake at (a) the Calaveras fault (CF) in NC and at (b) the San Jacinto fault (SJF) in SC. Other notations are the same as in Figure 2.

propagated to the southwest (positive value in Fig. 2) and then further intensified during the large-amplitude Rayleigh waves. This is consistent with the observations along the Parkfield–Cholame section of the SAF in CC (Peng *et al.*, 2008; Peng *et al.*, 2009), suggesting a similar triggering mechanism among these regions.

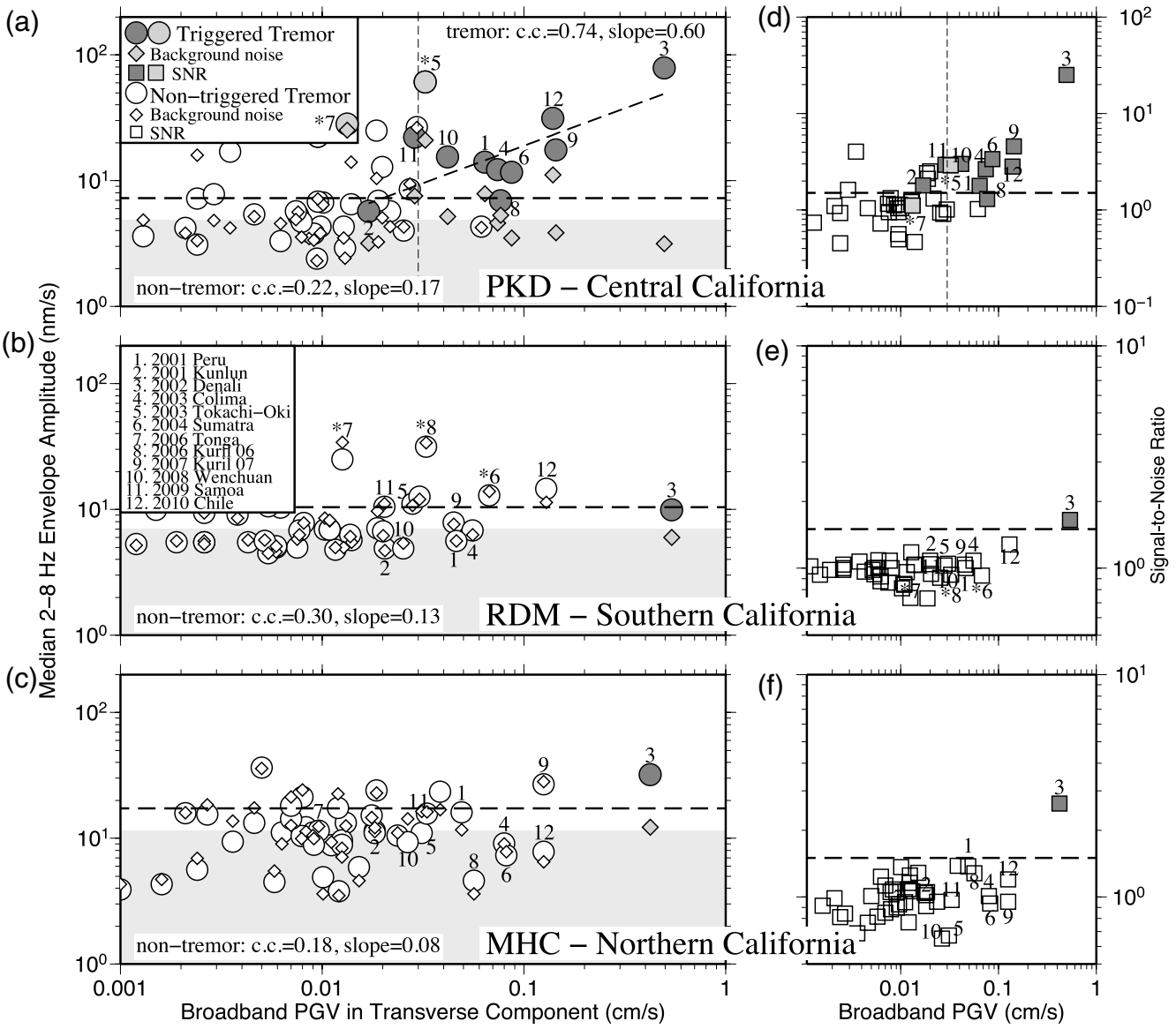

Figure 5. Maximum peak ground velocity (PGV) of surface wave (horizontal axis) in transverse component versus median amplitude (vertical axis) of the 2–8 Hz three-component band-pass-filtered envelope functions (a–c) during the surface waves and (d–f) signal-to-noise ratio (SNR) at broadband stations PKD, RDM, and MHC in central California (CC), southern California (SC), and northern California (NC), respectively. The event numbers preceded by an asterisk (*) indicate the measurement is from the nearby station FROB in CC and DNR in SC (Ⓔ Table S1, available as an electronic supplement to this paper). The tremor-triggering and nontriggering events were marked by shaded and open symbols, respectively. A total of 42 earthquakes were selected among the three regions. The numbers mark the measurements of 12 triggering events in CC. The background noise level of each event is calculated from a 600-s time window before the arrival of the predicted *P*-wave. The correlation coefficient (c.c.) and slope of the fitting line between the median tremor amplitudes and the PGVs for tremor and nontremor in each region are marked in (a–c). The light gray background shows the median noise level for all events. The horizontal dotted lines in (a–c) mark the 1.5 times of the median noise level in each region. The vertical dotted lines in (a, d) show the apparent triggering amplitude threshold of 0.03 cm/s in CC (Peng *et al.*, 2009). The horizontal dotted lines in (d–f) mark the 1.5 of the SNR.

Triggering Waves, Triggered Tremor, and Background Noise Level

To quantify the relationship between amplitudes of triggering waves and triggered tremor, we compared the PGV of teleseismic waves with the median amplitudes of the high-frequency signals during the arrival of large-amplitude surface waves, and pre-event noise (Chao *et al.*, 2012) recorded at the broadband stations PKD, RDM, and MHC in the CC, SC, and NC regions, respectively (Fig. 5). We computed the median amplitudes of both triggered tremor signals and nontriggering records from the three-component 2–8-Hz band-pass-filtered envelope functions, as well as the median amplitudes of noise during the 600-s before the predicted *P*-wave (or first *PKP*-type-wave) arrival. We adopted median,

rather than mean or maximum amplitude to suppress the impulsive signals generated by local earthquakes or other nontremor sources. In the cases when the signals during the surface waves were not well recorded at the three aforementioned stations, we measured the PGVs and amplitudes from nearby broadband stations instead (marked with asterisks in Fig. 5a,b; Ⓔ Table S1, available as an electronic supplement to this paper).

For the 10 (i.e., excluding two measurements from nearby stations) tremor-triggering events recorded at PKD in CC (Fig. 5a), we found a positive correlation between the median tremor amplitudes and the PGVs of the Love waves measured from the transverse component. The fitting line has a slope of 0.6 in log–log scale (correlation coefficient is 0.74), and the corresponding p-value equals 0.0144. The result indicates a 1.44% chance for the correlation between the x axis and y axis to be random, suggesting that the correlation is significant at more than 95% confidence level. In comparison, we found no evident correlation for the nontriggering events between PGVs of teleseismic surface waves and the median amplitudes of band-pass-filtered seismograms (with slope of 0.17, correlation coefficient of 0.22, and p-value of 0.2427). We measured the PGVs from the transverse components mainly because the tremor around the SAF shows higher correlations with the fault-parallel shear stresses induced by the Love waves (Peng *et al.*, 2009; Hill, 2010). A similar positive correlation is shown by the PGVs measured from the vertical component (Ⓔ Fig. S2, available as an electronic supplement to this paper). We also corrected for the effects of geometrical spreading and attenuation with a constant Q of 100 (Ⓔ Fig. S3, available as an electronic supplement to this paper), based primarily on the triggered tremor locations reported in Peng *et al.* (2009) (Ⓔ Table S2, available as an electronic supplement to this paper). For the triggered tremor since 2009 (namely the 2009 M_w 8.1 Samoa and 2010 M_w 8.8 Chile earthquakes), we used the centroid location from the triggered low-frequency earthquakes (Shelly *et al.*, 2011) during the arrival time of large-amplitude surface waves (Ⓔ Table S2, available as an electronic supplement to this paper). Ⓔ Figure S3 (available as an electronic supplement to this paper) shows that their correlations remain largely unchanged with and without corrections, mainly because the majority of the triggered tremor occurred near Cholame and their hypocentral distances to station PKD are similar.

Figure 5 shows that the median background noise levels for all events are 4.85, 6.95, and 11.5 nm/s in CC, SC, and NC, respectively. The smallest amplitude of the triggered tremor in CC is 5.7 nm/s (associated with the 2001 Kunlun earthquake), which is close to 1.5 times the median background noise level. We found that a signal-to-noise ratio (SNR) of 1.5 provides a reasonable threshold to separate most triggering events from nontriggering ones in the three regions (Fig. 5d–f). For events with lower SNR, the high-frequency tremor amplitude during the surface waves can be very close to the background noise level, which might interfere with the identification of possible triggered tremor.

Discussion and Conclusions

In this study we have systematically examined deep tremor triggered by large teleseismic earthquakes between 2001 and 2010 in three tectonically active regions along the SAF system. Our results revealed a marked difference in triggering behavior in California. In CC, 12 out of 42 large teleseismic events triggered tremor along the Parkfield–Cholame segment of the SAF. In comparison, only the 2002 Denali fault earthquake has triggered tremor around the CF in NC and the SJF in SC. In these two regions, the tremor was initiated by the Love waves and then intensified during the large-amplitude Rayleigh waves. In addition, tremor in this case occurred only when the particle velocity of the Love wave is to the southwest (positive value in Fig. 2), which produced right-lateral shear stress along the fault strike. The process is similar to that observed in CC (Peng *et al.*, 2008; Peng *et al.*, 2009). These observations suggest that triggered tremor in NC and SC was also the result of shear failure at depth driven by dynamic stresses from large-amplitude surface waves. Finally, the tremor amplitude has a positive correlation with the PGVs of the triggering waves in CC, further supporting the clock-advance model (Gomberg, 2010).

Because the PGVs of the triggering waves observed at three regions are similar, the associated dynamic stresses and deformation should be essentially the same. Hence, the variable triggering behavior observed in these regions could be largely attributed to background noise levels, background tremor rates, or frictional properties of the fault. As shown in Figure 5, the background noise levels measured at three broadband stations in each region are somewhat different. Station PKD in CC has the lowest background noise, while station MHC in NC has the highest. It is worth noting that the Parkfield–Cholame section of the SAF has high-quality and low-noise borehole sensors that are part of the High Resolution Seismic Network (HRSN). They are helpful in identifying triggered tremor with relatively weak signals in CC. However, the Plate Boundary Observatory (PBO) borehole stations were installed in SC after 2006. Although these stations have similar qualities to HRSN, they did not record any triggered tremor associated with the 23 teleseismic earthquakes (six of them triggered tremor in CC). For example, the 2010 Chile earthquake produced the second largest PGV but only triggered tremor in CC (Peng *et al.*, 2010), despite the fact that SC is slightly closer to the Chile mainshock and has larger PGV.

If we extrapolate the positive relationship between the PGVs and amplitudes of triggered tremor in CC to NC and SC, the maximum tremor amplitudes would be associated with the Denali fault event (Fig. 5b,c). In addition, the corresponding triggered tremor amplitudes for smaller PGVs in NC and SC would be much lower than the background noise

levels. Hence, even if tremor was triggered by teleseismic events other than the Denali fault earthquake in NC and SC, the tremor amplitude would be overwhelmed by the noise amplitude. In this case, the signals would not be coherent among different stations and would not be possibly identified by our visual inspection. In addition, if the pre-event noise level in CC is set to be that of NC, 6 out of the 12 observed triggering cases would become invisible. This

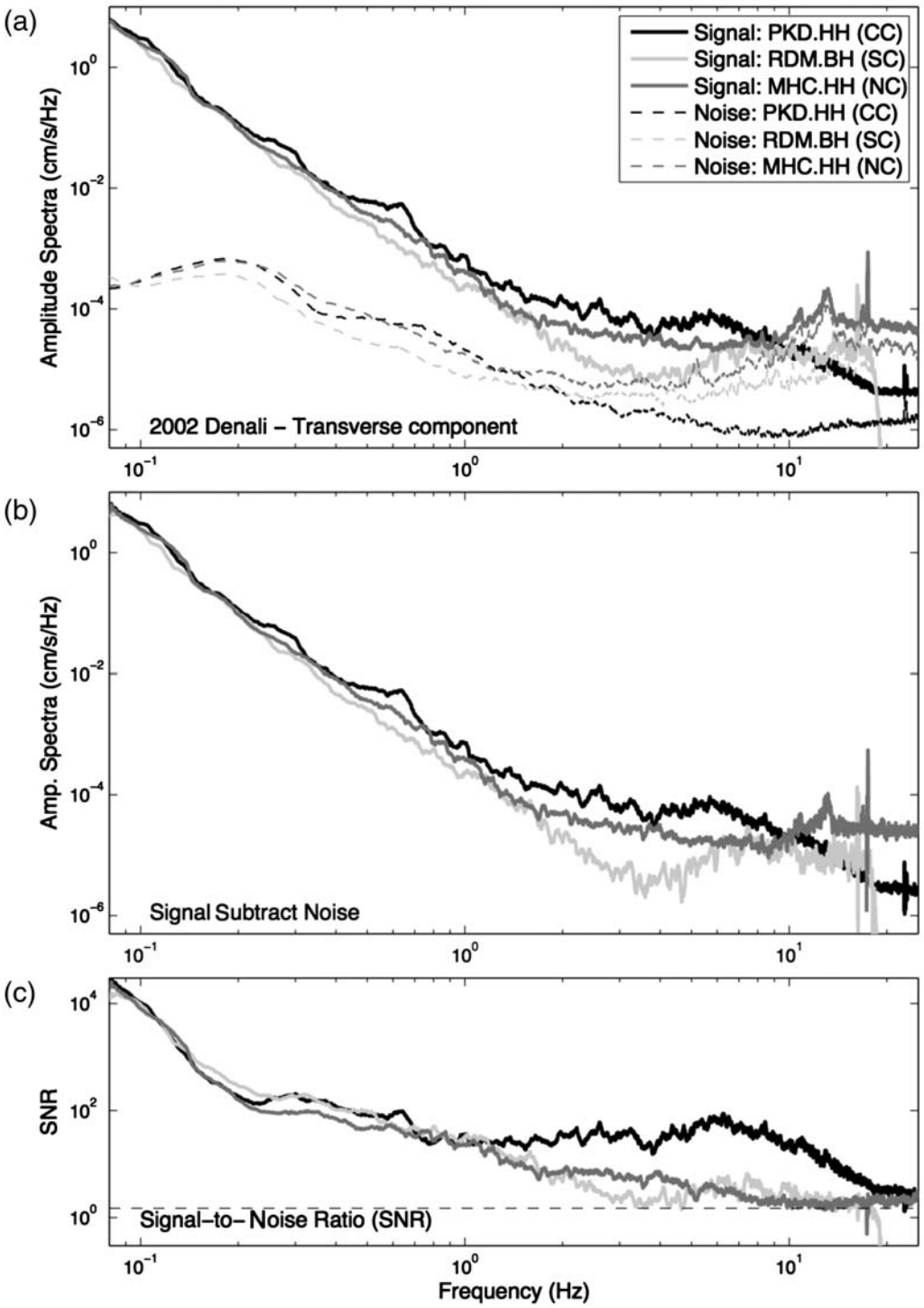

Figure 6. (a) Comparison of signal (solid line) and noise (dotted line) spectra in transverse velocity component at stations PKD in central California (CC), RDM in southern California (SC), and MHC in northern California (NC) for the 2002 Denali fault earthquake. The BH-channel (40-Hz sampling rate) data at RDM are used for computing the noise spectra due to lack of long-enough HH-channel (100-Hz sampling rate) data before the *P*-wave. (b) The spectral difference after subtracting the noise from the signal spectra. (c) The signal-to-noise ratio (SNR) spectra.

indicates that at least some difference in observations of triggering behavior is due to the background noise levels. Recent studies have shown that additional triggered tremor could be identified in NC and SC based on waveform matched filter techniques (Aguiar *et al.*, 2009; Brown, 2010). However, further analysis (A. Aguiar and J. Brown, personal comm., 2011) also revealed that the Denali fault earthquake was the only teleseismic earthquake that has triggered tremor in these regions. These results suggest that while additional triggered tremor may exist in NC and SC, their amplitudes are smaller and hence closer to or hidden by the background noises. In other words, it will require more advanced signal processing techniques to identify such signals if they exist.

It is worth noting that the maximum difference in the background noise levels at these regions is less than a factor of 3, which cannot explain a factor of 10 difference in the amplitude of tremor triggered by the Denali fault earthquake. To further demonstrate this, we compared the spectra during the surface waves of the Denali fault earthquake and the pre-event background noises in three regions (Fig. 6a). While the shape of the surface wave spectra in the frequency range of 0.01–0.2 Hz (5–100 s) are quite similar, the high-frequency signals (>2 Hz) are different in these regions. Hence, some differences were apparently caused by the different background noise. For example, station RDM appeared to record high background noise at frequencies of >10 Hz. However, even after we removed the contribution from the pre-event noise (assuming the noise spectra is stationary; Fig. 6b), we still found a factor of ~10 difference (Fig. 6c) in the spectra in the frequency range of tremor observation (2–8 Hz). The result again suggests that the background noise level likely contributes to, but is not the primary cause of, the different triggering behaviors.

In addition to background noise, the differences in tremor amplitudes could also be due to the path or site effects. For example, it is possible that in the frequency band of 2–8 Hz, the path and site effect in CC could amplify higher ground motions than in SC and NC. Because we did not have accurate path and site information in these regions, we randomly chose two microearthquakes in each region from the magnitude range of 1.5–2 within 10 km from the tremor source of the Denali fault earthquake in three regions (Ⓔ Table S3, available as an electronic supplement to this paper). These events were used as an empirical Green's function to demonstrate the path and site effects. The computed stress drops in CC and SC are compatible (Allmann and Shearer, 2007; Shearer *et al.*, 2006). Hence, we assumed that these events have similar source spectra. We computed the *S*-wave spectra for 10 s, starting 1 s before the *S*-wave arrivals, and the noise spectra for 10 s before the *P*-wave arrivals. Ⓔ Figure S4 (available as an electronic supplement to this paper) shows that the *S*-wave spectra around 2 Hz are compatible in three regions. The spectra at station RDM is higher for frequency $f > 10$ Hz, which is either due to the high background noise level or site amplification effects. In summary, the path and site effects also cannot completely explain the difference in tremor amplitudes for the frequency range of 2–8 Hz in these regions.

In addition to the amplitude of the triggering surface wave, another important parameter that controls the rate and amplitude of the triggered events is the unperturbed or background tremor rate (Gomberg 2010). Ambient tremor is very active in CC (Nadeau and Dolenc, 2005; Nadeau and Guilhem, 2009; Shelly *et al.*, 2011), while ambient tremor has not been detected with current instrumentation (J. P. Ampuero, personal comm., 2011). So far there have been no ambient tremor reports in NC. The fact that the ambient tremor activities in CC occur hourly to daily (Nadeau and Guilhem, 2009) indicates that many tremor patches could be on the verge of slipping and hence are prone to be triggered by the next coming large-amplitude surface waves. On the contrary, the lack of widespread ambient tremor in NC and SC suggests that either fewer tremor patches are ready to be triggered or that the patches need higher (longer) loading stress in order to reach their failure stage. Hence, the lack of widespread triggering of tremor in NC and SC is likely related to the low or absent background tremor rate in these regions.

The exact reason for different triggering and ambient tremor rates in these regions is still not clear (Peng and Gomberg, 2010; Beroza and Ide, 2011). Ellsworth (2008) suggested that triggered tremor in CC and NC might be associated with serpentinized fossil oceanic crust in these regions. However, such inference is rather speculative at this stage. Systematic searches for triggered and ambient tremor elsewhere, along with detailed analysis of the geophysical and material properties at tremor depth, are needed to further identify essential factors for tremor generation.

Data and Resources

Seismograms used in this study were downloaded from the Northern California Earthquake Data Center (http://www.ncedc.org/, last accessed May 2011) and the Southern California Earthquake Data Center (http://www.data.scec.org/, last accessed May 2011).

Acknowledgments

The seismic data were distributed by the Northern California Earthquake Data Center (NCEDC) and the Southern California Earthquake Data Center (SCEDC). The manuscript has benefited from comments by Iain Bailey, Joan Gomberg, David Hill, and an anonymous reviewer. K.C. and Z.P. were supported by the National Science Foundation (NSF) through awards EAR-0908310 and EAR-0956051 and by the Southern California Earthquake Center (SCEC). A.F. and L.O. were supported by the SCEC's Summer Intern Program. SCEC is funded by NSF Cooperative Agreement EAR-0106924 and U.S. Geological Survey Cooperative Agreement 02HQAG0008.

References

Aguiar, A. C., J. R. Brown, and G. C. Beroza (2009). Non-volcanic tremor near the Calaveras fault triggered by $M_w \sim 8$ teleseisms, *Eos Trans. AGU* **90,** no. 54, Fall Meet. Suppl., Abstract T23E-06.

Allmann, B. P., and P. M. Shearer (2007). Spatial and temporal stress drop variations in small earthquakes near Parkfield, California, *J. Geophys. Res.* **112,** no. B04305, doi 10.1029/2006JB004395.

Beroza, G. C., and S. Ide (2009). Deep tremors and slow quakes, *Science* **324,** 1025–1026, doi 10.1126/science.1171231.

Beroza, G. C., and S. Ide (2011). Slow earthquakes and nonvolcanic tremor, *Annu. Rev. Earth Planet. Sci.* **39,** 271–296, doi 10.1146/annurev-earth-040809-152531.

Brown, J. R. (2010). A catalog of low frequency earthquake activity from triggered tremor on the San Jacinto fault, abstract, *SCEC Annual Meeting*, Palm Springs, California, 11–15 September 2010, 198.

Chao, K., Z. Peng, C. Wu, C.-C. Tang, and C.-H. Lin (2012). Remote triggering of non-volcanic tremor around Taiwan, *Geophys. J. Int.* **188,** no. 1, 301–324, doi 10.1111/j.1365-246X.2011.05261.x.

Ellsworth, B. (2008). Nonvolcanic tremor beneath the San Andreas fault: Why?, *Aseismic Slip, Non-Volcanic Tremor, and Earthquakes Workshop*, Sidney, British Columbia, Canada, 25–28 February 2008, http://www.earthscope.org/es_doc/ETS/Talks/Ellsworth_ETS08_dunsmuir.pdf (last accessed January 2012).

Fabian, A., L. Ojha, Z. Peng, and K. Chao (2009). Systematic search of remotely triggered tremor in northern and southern California, *Eos Trans. AGU* **90,** no. 54, Fall Meet. Suppl., Abstract T13D-1916.

Ghosh, A., J. E. Vidale, Z. Peng, K. C. Creager, and H. Houston (2009). Complex nonvolcanic tremor near Parkfield, California, triggered by the great 2004 Sumatra earthquake, *J. Geophys. Res.* **114,** no. B00A15, doi 10.1029/2008JB006062.

Gomberg, J. (2010). Lessons from (triggered) tremor, *J. Geophys. Res.* **115,** no. B10302, doi 10.1029/2009JB007011.

Gomberg, J., J. L. Rubinstein, and Z. Peng (2008). Widespread triggering of nonvolcanic tremor in California, *Science* **319,** no. 173, doi 10.1126/science.1149164.

Guilhem, A., Z. Peng, and R. M. Nadeau (2010). High-frequency identification of non-volcanic tremor triggered by regional earthquakes, *Geophys. Res. Lett* **37,** L16309, doi 10.1029/2010GL044660.

Hill, D. P. (2010). Surface-wave potential for triggering tectonic (nonvolcanic) tremor, *Bull. Seismol. Soc. Am* **100,** no. 5A, 1859–1878, doi 10.1785/0120090362.

Miyazawa, M., and E. Brodsky (2008). Deep low-frequency tremor that correlates with passing surface waves, *J. Geophys. Res.* **113,** no. B01307, doi 10.1029/2006JB004890.

Miyazawa, M., and J. Mori (2006). Evidence suggesting fluid flow beneath Japan due to periodic seismic triggering from the 2004 Sumatra-Andaman earthquake, *Geophys. Res. Lett.* **33,** L05303, doi 10.1029/2005GL025087.

Nadeau, R. M., and D. Dolenc (2005). Nonvolcanic tremors deep beneath the San Andreas fault, *Science* **307,** no. 389, doi 10.1126/science.1107142.

Nadeau, R. M., and A. Guilhem (2009). Nonvolcanic tremor evolution and the San Simeon and Parkfield, California, earthquakes, *Science* **325,** 191–193, doi 10.1126/science.1174155.

Obara, K., H. Hirose, F. Yamamizu, and K. Kasahara (2004). Episodic slow slip events accompanied by non-volcanic tremors in southwest Japan, *Geophys. Res. Lett* **31,** L23602, doi 10.1029/2004GL020848.

Peng, Z., and J. Gomberg (2010). An integrated perspective of the continuum between earthquakes and slow-slip phenomena, *Nature Geosci.* **3,** 599–607, doi 10.1038/ngeo940.

Peng, Z., D. P. Hill, D. R. Shelly, and C. Aiken (2010). Remotely triggered microearthquakes and tremor in central California following the 2010 M_w 8.8 Chile earthquake, *Geophys. Res. Lett.* **37,** L24312, doi 10.1029/2010GL045462.

Peng, Z., J. E. Vidale, K. C. Creager, J. L. Rubinstein, J. Gomberg, and P. Bodin (2008). Strong tremor near Parkfield, CA, excited by the 2002 Denali fault earthquake, *Geophys. Res. Lett.* **35,** L23305, doi 10.1029/2008GL036080.

Peng, Z., J. E. Vidale, A. G. Wech, R. M. Nadeau, and K. C. Creager (2009). Remote triggering of tremor along the San Andreas fault in central California, *J. Geophys. Res.* **114,** no. B00A06, doi 10.1029/2008JB006049.

Rogers, G., and H. Dragert (2003). Episodic tremor and slip on the Cascadia subduction zone: The chatter of silent slip, *Science* **300,** 1942–1943, doi 10.1126/science.1084783.

Rubinstein, J. L., J. Gomberg, J. E. Vidale, A. G. Wech, H. Kao, K. C. Creager, and G. Rogers (2009). Seismic wave triggering of nonvolcanic tremor, episodic tremor and slip, and earthquakes on Vancouver Island, *J. Geophys. Res.* **114,** no. B00A01, doi 10.1029/2008JB005875.

Rubinstein, J. L., J. E. Vidale, J. Gomberg, P. Bodin, K. C. Creager, and S. D. Malone (2007). Non-volcanic tremor driven by large transient shear stresses, *Nature* **448,** 579–582, doi 10.1038/nature06017.

Shearer, P. M., G. A. Prieto, and E. Hauksson (2006). Comprehensive analysis of earthquake source spectra in southern California, *J. Geophys. Res.* **111,** no. B06303, doi 10.1029/2005JB003979.

Shelly, D. R., Z. Peng, D. P. Hill, and C. Aiken (2011). Triggered creep as a possible mechanism for delayed dynamic triggering of tremor and earthquakes, *Nature Geosci.* **4,** 384–388, doi 10.1038/ngeo1141.

Wang, T., and E. S. Cochran (2009). Study of triggered tremor characteristics and triggering threshold in Anza region, southern California, *Eos Trans. AGU* **90,** no. 54, Fall Meet. Suppl., Abstract T13D-1917.

School of Earth and Atmospheric Sciences
Georgia Institute of Technology
311 Ferst Drive
Atlanta, Georgia 30332
kevinchao@gatech.edu
(K.C., Z.P.)

Department of Earth and Ocean Sciences
University of South Carolina
701 Sumter Street
Columbia, South Carolina 29208
(A.F.)

Department of Geosciences
University of Arizona
1040 E. 4th Street
Tucson, Arizona 85721
(L.O.)

Manuscript received 18 May 2011